A DIELECTROPHORETIC CHAOTIC MIXER

Joanne Deval[(a)], Patrick Tabeling[(b)], Chih-Ming Ho[(a)]
[(a)]UCLA, MAE Dept, 420 Westwood Plaza, Los Angeles, California, 90095 USA
[(b)]Laboratoire de Physique Statistique de l'ENS, 24 rue Lhomond, 75231 Paris France

ABSTRACT

The time needed for achieving mixing in a micro bio-chemical system takes the major portion of the whole processing time. The characteristic length scale is so small that the flows are laminar, leaving mixing dependent solely on diffusion. We present a dielectrophoretic mixer which induces chaotic trajectories of embedded particles via a combination in space and time of electrical actuation and local channel geometry variation. Mixing time is therefore dramatically reduced. The design is kept very simple and fabrication is done using standard microfabrication techniques. Experimental observations and numerical simulations show the conditions in which chaotic trajectories can be achieved.

INTRODUCTION

The possibility of major time savings has been one of the main motivations for the miniaturization of detection devices. Many biological or chemical processes can now be achieved on microfluidic boards, where the typical channel width and height are generally between tens and hundreds of microns. 2D channels of this size generate laminar flows, where no instabilities can develop. This means that whenever two or more fluids merge, the only mixing mechanism is molecular diffusion, which demands long incubation times.

In the past, people have worked on diffusion time reduction by decreasing the characteristic length scale. e.g., channel subdivision [1], and 2D interface [2]. However, fabrication complexity and size constraints make them difficult to implement in biological fluidic boards. More recently, creating chaos using 3D passive geometry variation has been achieved in complex channels [3]. Another approach based on surface local 3D grooves has also been developed [4]. Generating chaotic advection via an external forcing was proposed in MEMS'97[5] and demonstrated in numerical simulations. In MEMS'01 [6], we showed how chaotic advection could be achieved using hydrodynamic forcing, and suggested an external time-varying force exerted onto embedded elements could also lead to chaotic trajectories. Here, we further develop this option, showing the efficacy of such a technique, via both experiments and simulation. Its simple design and fabrication facilitates its implementation and integration in a multi task fluidic board. Additionally, dielectrophoresis is already proven as a powerful tool in molecular manipulation [7,8] and is biocompatible.

DIELECTROPHORESIS

Dielectrophoresis (DEP) generally describes the polarization of an element relatively to its surrounding medium in a non-uniform electrical field, and the resulting motion. As detailed descriptions can be found in ref. [9,10], we will focus only on the translation motion due to DEP force. For a spherical particle of radius a, permittivity ε_p and conductivity σ_p, in a surrounding medium of permittivity ε_m, and conductivity σ_m, the dipole moment $\boldsymbol{m(\omega)}$ induced by the electrical field $\boldsymbol{E(\omega)}$, is given by the following equation:

$$\vec{m}(\omega) = 4\pi\varepsilon_m a^3 K(\omega)\vec{E} \qquad (1)$$

where the Clausius-Mossotti factor $K(\omega)$ is given by

$$K(\omega) = \frac{\varepsilon_p^* - \varepsilon_m^*}{\varepsilon_p^* + 2\varepsilon_m^*}, \qquad \varepsilon^* = \varepsilon - j\frac{\sigma}{\omega} \qquad (2)$$

The time-averaged DEP translation force $\boldsymbol{F(\omega)}$ can then be expressed as

$$\vec{F}(\omega) = 2\pi\varepsilon_m a^3 \Re e\left[K(\omega)\right]\vec{\nabla}E_{rms}^2 \qquad (3)$$

The Clausius-Mossotti factor can take any value between –1/2 and +1, which implies one can induce attractive or repulsive force by simply changing the frequency of the signal. As it varies with the dielectrical properties of both the medium and the particle, different populations of elements in a given medium under a given AC signal can exhibit opposite behaviors, as their frequency domains are different. A number of groups have already used these properties to separate particles or biological elements ([11],[12]).

We worked with polystyrene particles in aqueous medium, whose conductivity was adjusted in the range of 10-20mS/m. We found the cross-over frequency in the order of a few MHz. High frequencies generate a negative DEP force, where particles are repelled from electrode edges, while at lower frequencies positive DEP forces move the particles to the electrode edges, as they correspond to highest field gradients. We worked with a ±10V AC signal that alternated between 700kHz and 15MHz at a rate of 1 Hz.

Appropriate spatial non-uniformity of the field is critical in achieving strong translation motions. We are using the CFD-ACE+ code from CFDRC to analyze the electrical field distribution and optimize the electrode design. As shown by (3), the DEP force is proportional to the gradient of $\boldsymbol{E^2}$. Figure 1 shows the 2D distribution of $\boldsymbol{E^2}$

in a configuration where electrodes are located on the cavity boundaries. The rapid decrease with distance encourages the design of electrodes that extend into the fluid mainstream, so that particles with highest velocities can be affected by the DEP force.

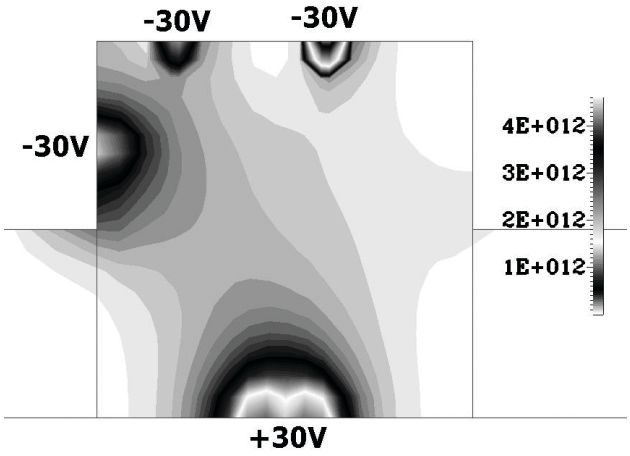

Figure 1: 2D distribution of E^2 in V^2/m^2 in a 100umx100um side well.

CHAOS

Chaotic regimes have been mostly described in macro-scale flows [13], and chaotic advection was particularly investigated as a way to enhance mixing efficiency [14]. One of its critical features is that two particles initially located close to each other will exponentially separate from one another in time. Inducing chaotic trajectories onto the particles will therefore homogenize their distribution across the entire channel.

Chaos cannot occur in 2D steady laminar flows. A third dimension is needed, whether it comes for spatial 3D variation (as developed by people working on passive 3D chaotic flow), or from some external forcing varying in time. The Stokes equation is linear. Non-linearity is necessary in the equation of motion of the particle, and is introduced by an external force applied onto the particle. We are applying a dielectrophoretic force that varies in space and time onto particles whose motion is otherwise given by flow field, and thus can create the conditions for chaotic trajectories to occur.

However, non-linearity is necessary but not sufficient, and chaos characterization requires studies to properly categorize it. Moreover, some chaotic regimes may not be efficient on a short-time basis unless the number of mixing units is multiplied, which then would make the device non-realistic. To simplify our approach, we are focusing on two main objectives: experimentally, we want to generate folding and stretching of the particle distribution after one or two cavities, while computationally we wish to model and analyze the system in a longer time range to extract its properties.

DIELECTROPHORETIC MIXER FABRICATION

The fabrication process steps are shown in Figure 2. Thermal oxidation and LPCVD nitride deposition are first performed on a silicon wafer. The backside holes are patterned into the nitride layer before a through-wafer KOH etch is done. Electrodes are then patterned in chromium/gold layers via lift-off. A PECVD nitride layer is deposited to ensure isolation and avoid electrolysis.
The channels and chambers structure is then patterned in a 25um thick SU8-25 photoresist layer. A thin cover glass (Fisher Premium microslides) is then bonded to close the channel via a thin (~3um) SU8-5 layer.

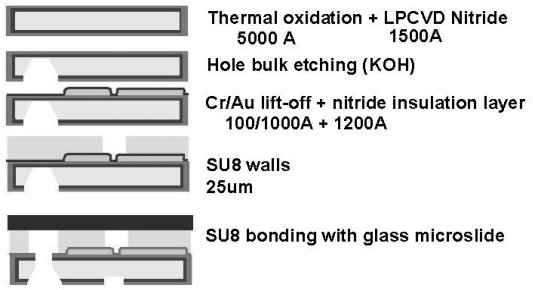

Figure 2: Micromixer fabrication process

One of the designs we experimented is shown in Figure 3. It consists of the successive side wells, located on opposite sides of the main channel, which is 50um wide. Each of them displays four distinct electrodes at the bottom. Visualization is performed using Bausch&Lomb MicroZoom™ microscope, while AC voltage is applied to selected electrodes by a Hewlett-Packard 33120A function generator. Fluid flow is controlled by a Harvard Apparatus mode l"44" syringe pump connected to the outlet, while each inlet holes is connected to reservoirs via peek™ tubing.

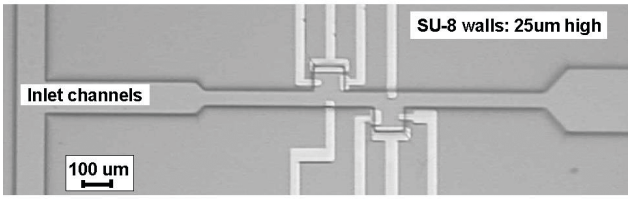

Figure 3: Top view of the micromixer test section

EXPERIMENTAL RESULTS

Successive snapshots of the particle positions over a period of total 2s are shown in Figure 4. As the particles enter the first cavity, positive DEP pulls them into the low velocity region, attracted by the electrode 1. As the frequency switches, they are repelled from the electrode 1 edges, and particles in the main stream of the flow are dragged downstream by the fluid. As the frequency switches back to the positive domain, incoming particles are attracted upwards, while a folding is created in the cavity as the particles far from the electrode experience a force too small to overcome fluid drag. The combination

of the two opposite motions generates folding and stretching and greatly accelerates the homogenization of the particle distribution. Folding and streching are the physical mechanisms to produce a non-zero Lyapunov exponent. Note the particle distribution at the channel exit in the last snapshot corresponds to an initial location in the upper half of the channel.

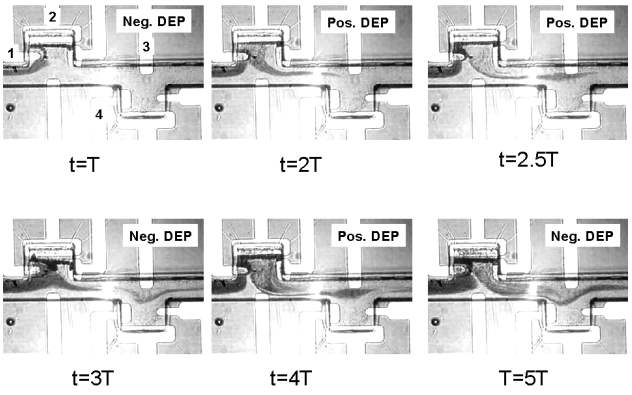

Figure 4: ±10V AC voltage is applied between electrodes 1 and 2 and between 3 and 4. AC Frequency switches between 700kHz (positive DEP domain) and 15MHz (negative DEP domain) at a rate of T=0.5s.

The dielectrophoretic force greatly decreases with distance from the electrode edge. As shown in [10], the force magnitude close to the edge reaches values much stronger than other typical particle forces at this scale. In other words, once the particle is "trapped" by positive DEP, strong fluid velocity is needed to generate sufficient drag to overcome this force. Conversely a negative DEP is required to repel particles attracted to electrode edges when these are located in a low velocity region, such as the upper part of the cavity. One can actually notice that in the observation shown in Figure 4, some trapping occurs at electrode 2 as negative DEP does not send some particles far enough. Also, fluid velocity must be kept low (in the order of hundreds of microns per second) to allow the DEP force to overcome the fluid drag (for voltages in the order of ±10 Volts and gaps in the order of 10 to 20 microns).

NUMERICAL SIMULATIONS

As dielectrophoretic forces decreases quickly with distance and our electrodes are located at the bottom of the channel, we considered the system to be two-dimensional. The particle motions are therefore studied in the horizontal plane, and the experimentally observed vertical motion is therefore neglected. However, this model emphasizes the interaction between flow velocity field and external forcing, which is the starting point of our approach.

Because of code requirements, the electrodes must be located on the boundaries of the flow channel. Particles position is computed after solving the Lagrangian equation of motion given by:

$$m\frac{d\vec{v}}{dt} = C_d\rho(\vec{U}-\vec{v})\left|U-v\right|\frac{A_d}{2} + \text{body\_force} \qquad (4)$$

where m and v are the particle mass and velocity, U and ρ the fluid velocity and density. C_d and A_d respectively refer to the drag coefficient and the droplet frontal area. The only body force which is taken in account is DEP force, as we neglect gravity.

Depending on the combination of fluid velocity and electrical field actuation frequency, the distortion of the particle distribution could follow three main patterns. First, the external force is large, and particles are finally accumulated on a single line almost in the middle of the main stream, while some others are indefinitely trapped in the cavities (see Figure 5). Second, the force is small, and the particle motion is hardly perturbed, and small waves can be seen on the interface between different population. Lastly, and most useful, particles distribution undergoes a series of stretching and folding as fluid drag is overcome or is reinforced by positive DEP or negative DEP (see Figure 6)

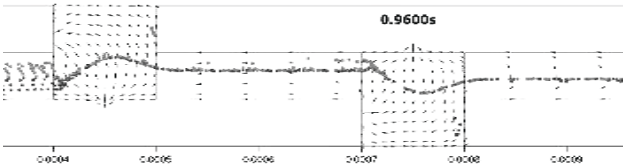

Figure 5: negative DEP repel particles on a single line. Channel is 50um wide, and side wells are 100um long. Arrows represent electrical field distribution.

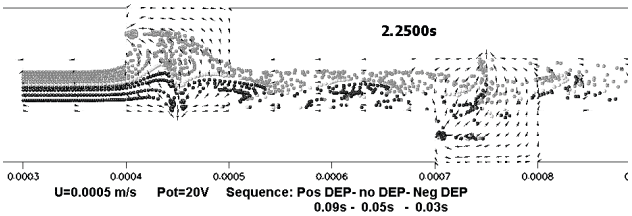

Figure 6: lower half particles meet upper half particles as folding and stretching occur throughout the cavities

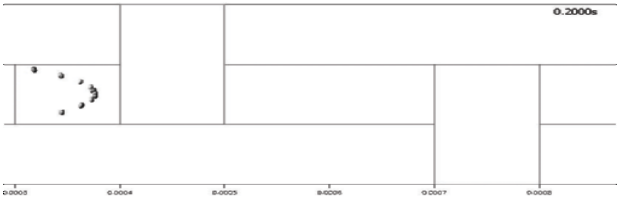

Figure 7: the initial vertical distribution of pairs of particles is distorted by Poiseuille flow before entering the test section. Each point corresponds to a pair of particles very close to each other.

We computed the stretching rate for different sets of particles when they flow past the two cavities under the actuation scheme described in Figure 6. We followed the trajectories of 11 pairs of particles distributed along a vertical line, as shown in Figure 7.

As shown in Figure 8, the external forcing creates a much stronger stretching rate that simple Poiseuille flow. Moreover, Poiseuille flow stretches particle distribution in only one direction, and does not cause different layers to interfere. The external forcing separates each pair of particles, as the pair enters the cavity and is submitted to the electrical field. After passing through the two cavities, the Poiseuille stretching dominates, and the stretching rate looks like the no-actuation case.

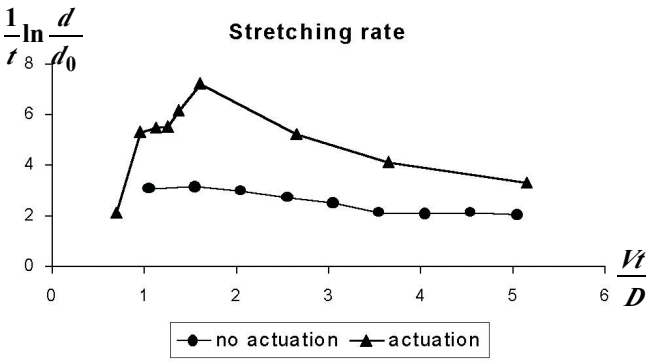

Figure 8: Stretching rate averaged over the 11 pairs with and without actuation. V=inlet velocity. D=cavity length. d and d_0 are the particle pair separation distance at time t and t_0. Index value between 1 and 2 corresponds to the first cavity region for most of the particles.

DISCUSSION

Both the experiments and the numerical simulations revealed the necessity to create saddle points. Saddle points refer to the mathematical definition of bifurcation in dynamical systems. Particles entering this region undergo a sequence of stretching in one direction and compressing in the other direction which finally guarantees an exponential stretching rate. An appropriate electrical field distribution that can pull particle sets into a quasi no-velocity region can achieve such conditions. A set of particles can then be folded and stretched around a virtual quasi-static point by the combination of external forcing (DEP force) and drag (due to fluid velocity field). Additional numerical simulations are under progress to understand how the different regimes depend on the actuation amplitude, the actuation frequency and the fluid velocity. Different cavity geometry and electrode distributions are also being investigated.

CONCLUSION

We developed a simple and efficient micromixer which can easily be integrated in a microfluidic board and adapted to different fluids, reagents, or biological components. The channel geometry is simple, and fabrication remains straightforward, as it only needs an array of microelectrodes integrated in the channel. It takes advantage from the relatively high magnitude of dielectrophoretic force compared to other forces acting on micron and submicron particles. When the electrical field is appropriately combined in time and space with the velocity flow field, saddle point regions are generated, where particle sets are stretched and folded around a virtual quasi-static point. Chaotic trajectories can be induced onto the particles, leading to fast and efficient mixing.

ACKNOWLEDGMENTS

This project funding was provided by DARPA/MTO BioFlips program under contract No. N66001-00-C8092. The authors would like to thank Dr Zhijang Chen from CFRDC for his help with the DEP modulus.

REFERENCES

1 J. Branebjerg, P. Gravesen, J.P. Krog, C.R. Nielsen, MEMS'96, pp.441–446.
2 R. Miyake, T.S.J. Lammerink, M. Elwenspoek, J.H.J. Fluitman, IEEE'93, pp. 248–253.
3 R. H. Liu et al., J. of MEMS., 9, (no.2), IEEE, June 2000, pp.190-197.
4 G.M. Whitesides, A.D. Stroock, Physics Today 54(2001), pp. 42-48.
5 J. Evans, D. Liepmann, A.P. Pisano, MEMS '97, pp. 96-101.
6 Y.-K. Lee, J. Deval, P. Tabeling, C.-M. Ho, MEMS'01, pp.483-486.
7 R. Pethig, G.H. Markx, Trends In Biotechnology, 1997 Oct, V15 N10:426-432.
8 M.P. Hughes, Nanotechnology, 2000 Jun, V11 N2:124-132.
9 X.B.Wang; Y.Huang; F.F. Becker; P.R.C. Gascoyne, J. of Phys. D-App.Phys., 1994 Jul 14,V27N7:1571-1574.
10 A. Ramos, H. Morgan, N.G. Green, A. Castellanos, J. of Phys. D-App. Phys., 1998 Sep 21,V31N18:2338-2353.
11 X.B. Wang, J. Yang, Y. Huang, J. Vykoukal, and others, Anal. Chem., 2000 Feb 15, V72 N4:832-839.
12 N.G. Green, H. Morgan, J. of Physics D-Applied Physics, 1997 Jun 7, V30 N11:L41-L44.
13 J.M. Ottino, Cambridge University Press, 1989.
14 H. Aref, J. Fluid Mech., 1984, 143:1–21.